Theory of Two-Dimensional Turbulent Wakes

S. C. LEE* AND J. E. AUILER†
University of Missouri, Rolla, Mo.

Nomenclature

a_1 = constant in relation between turbulent shear and turbulent kinetic energy
a_2 = constant in turbulent kinetic energy dissipation relation
d = diameter of cylinder
D_k = turbulent kinetic energy dissipation
k = turbulent kinetic energy
l_k = mixing length for turbulent kinetic energy
R = radius of cylinder
u,v = mean velocity components
U_0 = freestream velocity
u',v',w' = fluctuating turbulent velocity components
x,y = independent coordinates
ϵ = eddy viscosity
ρ = density
σ_k = turbulent kinetic energy quantity analogous to Prandtl number for total mean flow energy
θ_0 = momentum thickness at trailing edge of flat plate
τ = turbulent shear stress
ν = kinematic viscosity
$\langle\ \rangle$ = indicates time average of quantity

Introduction

STUDIES of the characteristics of turbulent wakes are considered necessary in order to more fully understand the hydrodynamic effect on the collision coalescence mechanism between freely falling droplets in atmospheric clouds. The collision coalescence mechanism is one of the prominent processes by which precipitation elements are formed from cloud droplets. However, no experimental results are available for axisymmetric turbulent wakes for the purpose of developing the analytical method. As the first step in extending the analytical solution to the case of axisymmetric wakes, the analytical method is compared with available experimental results for two dimensional wakes.

Analysis

The consideration of turbulence energy in free mixing studies was conducted by Lee and Harsha.[1] Application of this method in two-dimensional turbulent wakes may be outlined as follows:

Continuity

$$(\partial \rho u/\partial x) + (\partial \rho v/\partial y) = 0 \tag{1}$$

where ρ is the density, and u and v are the mean velocity components in the x and y directions, respectively.

Momentum

$$\rho u(\partial u/\partial x) + \rho v(\partial u/\partial y) = (\partial/\partial y)[\epsilon(\partial u/\partial y)] \tag{2}$$

where ϵ is the so-called eddy viscosity and is defined as

$$\epsilon = \tau/(\partial u/\partial y) = -\langle(\rho v)'u'\rangle/(\partial u/\partial y) \tag{3}$$

with the primes denoting the fluctuating quantities and the symbol $\langle\ \rangle$ denoting time average value.

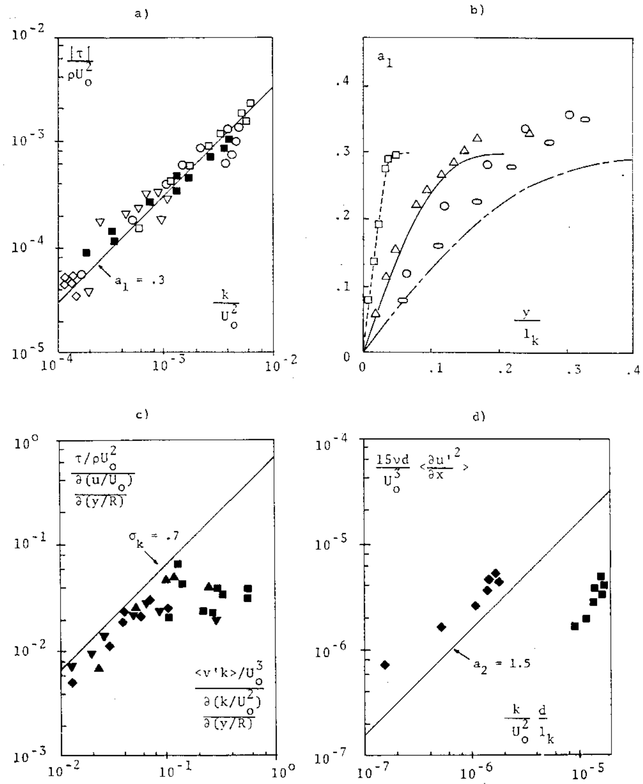

Fig. 1. Comparison between analytical models and experimental data. a) Correlation between local turbulent shear stress and local turbulent kinetic energy [Eq. (6)]. b) Comparison between Eq. (6a) and experimental data near the axis of symmetry. c) Correlation of parameters associated with diffusion of turbulent kinetic energy [Eq. (7)]. d) Correlation between dissipation of turbulent kinetic energy and local turbulent kinetic energy [Eq. (8)].

Turbulent kinetic energy

$$\rho u \frac{\partial k}{\partial x} + \rho v \frac{\partial k}{\partial y} = \frac{\partial}{\partial y}\left[\frac{\epsilon}{\sigma_k}\frac{\partial k}{\partial y}\right] + \epsilon\left(\frac{\partial u}{\partial y}\right)^2 - D_k \tag{4}$$

where k is the turbulent kinetic energy and is defined as

$$k = \tfrac{1}{2}\{\langle u'^2\rangle + \langle v'^2\rangle + \langle w'^2\rangle\} \tag{5}$$

The relation between the local turbulent kinetic energy and the local turbulent shear stress has been assumed as

$$\tau = a_1\rho k(\partial u/\partial y)/|\partial u/\partial y| \tag{6}$$

where a_1 is a proportionality constant, and the velocity gradient ratio designates that the shear stress has the same sign as the local velocity gradient. Correlation of Chevray and Kovasznay's[2] experiments on wakes behind a flat plate and Townsend's[3] and Kobashi's[4] experiments on wakes behind cylinders indicated that $a_1 = 0.3$ for most of the mixing region, as shown in Fig. 1a. Along the axis of symmetry the shear stress reduces to zero while the turbulent kinetic energy remains nonzero. An approximation for a_1 in the vicinity of the axis of symmetry was used by Lee and Harsha[1] as

$$a_1 = 0.3|\partial u/\partial y|/|\partial u/\partial y|_{\max} \tag{6a}$$

where $|\partial u/\partial y|_{\max}$ is the maximum velocity gradient at the desired x location. Fig. 1b indicates the approximation as compared with Chevray and Kovasznay's[2] experiment.‡ Table 1 explains the symbols used in all figures.

The exchange coefficient for the diffusion term of the tur-

Received January 20, 1970; revision received April 6, 1970. Research supported by the Office of Naval Research, THEMIS Contract N00014-68-A-0497.

* Assistant Professor of Mechanical and Aerospace Engineering. Member AIAA.
† Graduate Research Assistant. Student Member AIAA.

‡ Note that the ordinate of Figs. 1 and 2 of Ref. 2 should be multiplied by 10^{-2}, an obvious oversight.

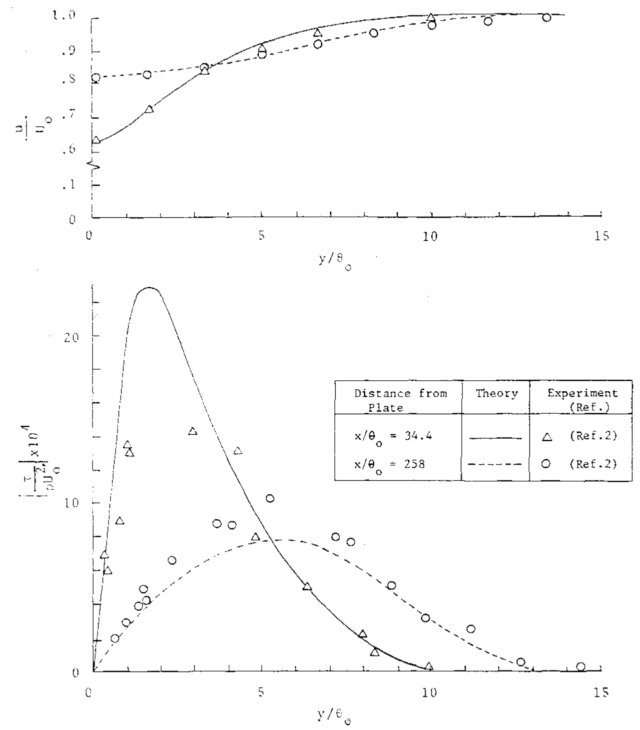

Fig. 2. Shear and mean velocity distributions in the wake of a flat plate.

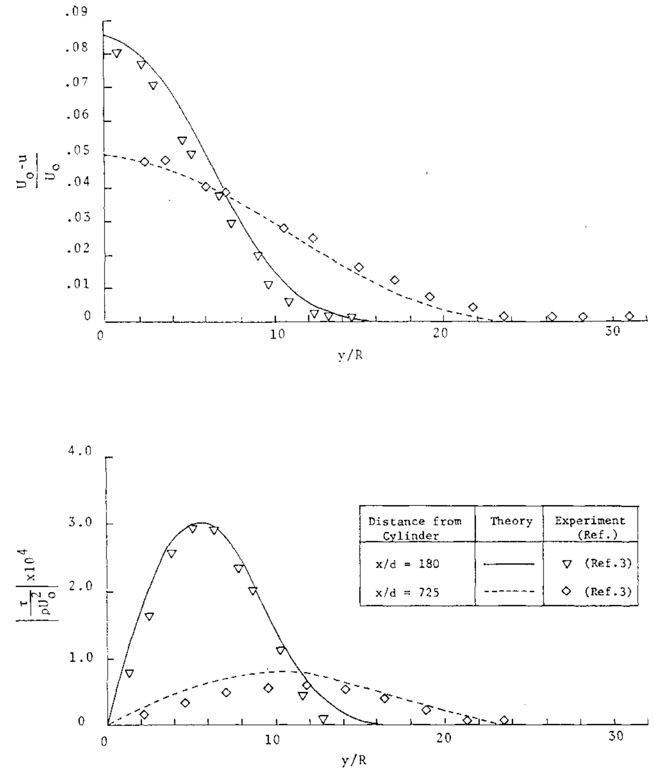

Fig. 3. Shear and mean velocity distributions in the wake of a cylinder.

bulent kinetic energy J_k may be expressed as

$$\epsilon/\sigma_k = J_k/(\partial k/\partial y) = -\langle(\rho v)'k\rangle/(\partial k/\partial y) \quad (7)$$

with σ_k analogous to the turbulent Prandtl number, as described by Patankar and Spalding.[5] Correlation of Townsend's[6] and Kobashi's[4] experiments on energy diffusion is shown in Fig. 1c in comparison with the value of $\sigma_k = 0.7$ used in this study.

No dissipation measurements are available in nonisotropic turbulence. The isotropic turbulence data presented by Townsend[6] and Kobashi[4] were compared with the dissipation model as suggested by Patankar and Spalding[5] and used by Lee and Harsha,[1]

$$D_k = a_2\rho k^{3/2}/1_k \quad (8)$$

where a_2 is a proportionality constant and 1_k is the half width of the mixing region. A comparison between the numerical value of $a_2 = 1.5$ used in this analysis and the isotropic turbulence measurements is shown in Fig. 1d.

The detailed analytical procedure used in this study for obtaining numerical solutions was discussed by Lee and Harsha[1] and by Spalding and Patankar.[7] The resulting shear and

Table 1 Explanation of figures

Geometry	Location	Symbols representing experimental data (Reference)	For Fig. 1b only Eq. (6a) $a_1 = 0.3 \left\lvert\frac{\partial u}{\partial y}\right\rvert \Big/ \left\lvert\frac{\partial u}{\partial y}\right\rvert_{max}$
Flat plate	$x/\theta_0 = 8.6$	□ (Ref. 2)	----
Flat plate	$x/\theta_0 = 34.4$	△ (Ref. 2)	———
Flat plate	$x/\theta_0 = 258$	○ (Ref. 2)	—.—
Flat plate	$x/\theta_0 = 414$	○ (Ref. 2)	
Cylinder	$x/d = 42$	■ (Ref. 4)	Remark: experimental data in Fig. 1b represents $a_1 = \tau/\rho k$
Cylinder	$x/d = 80$	▲ (Ref. 4)	
Cylinder	$x/d = 120$	▼ (Ref. 6)	
Cylinder	$x/d = 160$	◆ (Ref. 6)	
Cylinder	$x/d = 180$	▽ (Ref. 3)	
Cylinder	$x/d = 725$	◇ (Ref. 3)	

mean velocity profiles were compared with the experiments for two dimensional turbulent wakes performed by Chevray and Kovasznay[2] and Townsend.[3]

Results and Discussion

Figure 2 shows the comparison between the present analytical solution and Chevray and Kovasznay's[2] experimental results for turbulent wakes behind a flat plate. The mean velocity is nondimensionalized by the freestream velocity U_0, and the distance normal to the freestream velocity is nondimensionalized by the momentum thickness at the trailing edge of the flat plate θ_0. Very good agreement was reached for mean velocity distributions for all locations in the x direction. The test data presented represent measured results on one side of the wake since the wake is symmetric. The shear stress distributions were compared with the experimental results of both sides of the symmetric wake in order to consider possible data scattering. It is noted that the analytical solution over predicted the maximum shear at $x = 34.4\ \theta_0$, and under predicted the maximum shear at $x = 258\ \theta_0$. Nevertheless, the agreement can be considered satisfactory for most engineering applications.

Figure 3 shows the comparison between the present analytical solution and Townsend's[3] experimental results for the far wake region downstream of a circular cylinder. The nondimensionalized velocity as used by Townsend is based on the difference between the freestream and the mean wake velocities. The nondimensionalized distance normal to the flow direction is based on the radius of the cylinder while the nondimensionalized distance in the flow direction is based on the diameter of the cylinder. The test data presented for both mean velocity and shear represent measured results on one side of the wake. The agreement again appears to be very good for both mean velocity and shear stress distributions.

Based on Fig. 1, the numerical values used for coefficients a_1, σ_k and a_2 seem to be questionable. In order to evaluate the effect of these coefficients on mean velocity and shear stress distributions, a parametric study was made using various combinations of a_1, σ_k and a_2, allowing a_1 to vary from 0.2 to 0.3, σ_k from 0.4 to 0.7 and a_2 from 1.0 to 2.4. The results indicated that the centerline mean velocity changed by less than 10% and the maximum shear changed by approximately 30%.

Conclusion

The use of the turbulent kinetic energy equation reduces the uncertainty introduced by the phenomenological model of eddy viscosity. The coefficients of $a_1 = 0.3$, $\sigma_k = 0.7$ and $a_2 = 1.5$ provide reasonable predictions for most of the studied engineering problems. However, detailed turbulence measurements are very much needed if the turbulence energy approach can be of any significance in contributing to the basic understanding of the turbulence phenomenon.

References

[1] Lee, S. C. and Harsha, P. T., "The Use of Turbulent Kinetic Energy in Free Mixing Studies," AIAA Paper 69-683, San Francisco, Calif., 1969.

[2] Chevray, R. and Kovasznay, L. S. G., "Turbulence Measurements in the Wake of a Thin Flat Plate," *AIAA Journal*, Vol. 7, No. 8, Aug. 1969, pp. 1641–1642.

[3] Townsend, A. A., "Measurements in the Turbulent Wake of a Cylinder," *Proceedings of the Royal Society*, London, Ser. A, Vol. 190, 1947, pp. 551–561.

[4] Kobashi, Y., "Measurements of Pressure Fluctuation in the Wake of a Cylinder," *Journal of the Physical Society of Japan*, Vol. 12, 1957, pp. 533–543.

[5] Patankar, S. V. and Spalding, D. B., "A Finite-Difference Procedure for Solving the Equations of the Two-Dimensional Boundary Layer," *International Journal of Heat and Mass Transfer*, Vol. 10, 1967, pp. 1389–1411.

[6] Townsend, A. A., "Momentum and Energy Diffusion in the Turbulent Wake of a Cylinder," *Proceedings of the Royal Society*, London, Ser. A, Vol. 197, 1949, pp. 124–140.

[7] Spalding, D. B. and Patankar, S. V., *Heat and Mass Transfer in Turbulent Boundary Layers*, CRC Press, Cleveland, 1968.

Relative Motion of Two Particles in Elliptic Orbits

E. R. Lancaster*
NASA Goddard Space Flight Center, Greenbelt, Md.

Nomenclature

$\mathbf{r}$ = position vector at time t, $r = |\mathbf{r}|$
$\mathbf{v}$ = velocity vector at time t, $v = |\mathbf{v}|$
E = eccentric anomaly at time t
a = semimajor axis, $b = 1/a$, $c = a^{1/2}$
k^2 = μ = gravitational constant
$\mathbf{r}\cdot\mathbf{v}$ = scalar product of $\mathbf{r}$ and $\mathbf{v}$

OVER the past decade a number of papers[1–6] have presented approximate solutions to the problem of the relative motion of two particles in elliptic orbits in an inverse-square central force field. These papers have assumed that the relative position and velocity vectors are quite small compared to the position and velocity vectors of the particles, and several have further assumed one of the particles to be in a circular[1,2] or nearly circular[3,4] orbit. We derive below an exact solution to this problem, subject to no restrictions. The results have applications to problems of rendezvous, nonlinear error analysis, station keeping, targeting, surveillance, and satellite clustering.

Received April 30, 1970.
* Aerospace Engineer.

Solution

Kepler's equation for elliptic motion and the updating equations for position and velocity can be written in the form[7]

$$T = C + A(1 - \cos C) - B \sin C \quad (1)$$

$$\mathbf{r} = [1 - H(1 - \cos C)]\mathbf{r}_0 + [D(1 - \cos C) + N \sin C]\mathbf{v}_0 \quad (2)$$

$$\mathbf{v} = -(P \sin C)\mathbf{r}_0 + [1 - S(1 - \cos C)]\mathbf{v}_0 \quad (3)$$

where

$$A = \mathbf{r}_0\cdot\mathbf{v}_0/(kc),\ B = 1 - r_0 b,\ T = ktb/c$$

$$H = a/r_0,\ D = a(\mathbf{r}_0\cdot\mathbf{v}_0)/\mu,\ N = r_0 c/k$$

$$P = kc/(rr_0),\ S = a/r,\ C = E - E_0$$

and a zero subscript indicates the value at time 0.

Let subscript 1 on a symbol designate the value of that symbol for particle 1 in orbit 1 and subscript 2 the value for particle 2 in orbit 2. We define

$$\gamma = C_2 - C_1,\ \boldsymbol{\varepsilon} = \mathbf{r}_2 - \mathbf{r}_1,\ \boldsymbol{\lambda} = \mathbf{v}_2 - \mathbf{v}_1,\ \tau = T_2 - T_1$$

$$\alpha = A_2 - A_1$$

$$\beta = B_2 - B_1,\ \eta = H_2 - H_1,\ \delta = D_2 - D_1,\ \nu = N_3 - N_1$$

$$\rho = P_2 - P_1,\ \sigma = S_2 - S_1$$

If we place a subscript 1 on all symbols in Eqs. (1–3) and subtract the resulting equations from the set with subscripts 2 on all symbols, we obtain

$$T' = \gamma + A'(1 - \cos\gamma) - B' \sin\gamma \quad (4)$$

$$\boldsymbol{\varepsilon} = (1 - H_1F)\boldsymbol{\varepsilon}_0 + (D_1F + N_1G)\boldsymbol{\lambda}_0 - (H_2Q + \eta F)\mathbf{r}_{20} + (D_2Q + \delta F + N_2R + \nu G)\mathbf{v}_{20} \quad (5)$$

$$\boldsymbol{\lambda} = -P_1G\boldsymbol{\epsilon}_0 + (1 - S_1F)\boldsymbol{\lambda}_0 - (P_2R + \rho G)\mathbf{r}_{20} - (S_2Q + \sigma F)\mathbf{v}_{20} \quad (6)$$

where we have defined

$$F = 1 - \cos C_1,\ G = \sin C_1 \quad (7)$$

$$T' = \tau + \beta G - \alpha F \quad (8)$$

$$A' = A_2 \cos C_1 + B_2 \sin C_1 \quad (9)$$

$$B' = B_2 \cos C_1 - A_2 \sin C_1 \quad (10)$$

$$Q = \cos C_1(1 - \cos\gamma) + \sin C_1 \sin\gamma \quad (11)$$

$$R = \cos C_1 \sin\gamma - \sin C_1(1 - \cos\gamma) \quad (12)$$

To obtain equations for α, β, τ, η, δ, ν, ρ, and σ which do not suffer a loss of significant digits due to the subtraction of nearly equal numbers, we proceed as follows:

$$kcA = \mathbf{r}_0\cdot\mathbf{v}_0$$

$$k(c_2A_2 - c_1A_1) = \mathbf{r}_{20}\cdot\mathbf{v}_{20} - \mathbf{r}_{10}\cdot\mathbf{v}_{10}$$

$$k[c_2(A_2 - A_1) + A_1(c_2 - c_1)] = \mathbf{r}_{20}\cdot\mathbf{v}_{20} - \mathbf{r}_{10}\cdot\mathbf{v}_{10}$$

The last equation can be solved for α. Equations for the other quantities can be obtained in a similar manner. The full set follows:

$$kc_2\alpha = \mathbf{r}_{20}\cdot\mathbf{v}_{20} - \mathbf{r}_{10}\cdot\mathbf{v}_{10} - kA_1(c_2 - c_1) \quad (13)$$

$$\beta = r_{10}(b_1 - b_2) - b_2(r_{20} - r_{10}) \quad (14)$$

$$c_2\tau = -kt(b_1 - b_2) - T_1(c_2 - c_1) \quad (15)$$

$$r_{10}\eta = a_2 - a_1 - H_2(r_{20} - r_{10}) \quad (16)$$

$$\mu\delta = a_2(\mathbf{r}_{20}\cdot\mathbf{v}_{20} - \mathbf{r}_{10}\cdot\mathbf{v}_{10}) + (a_2 - a_1)\mathbf{r}_{10}\cdot\mathbf{v}_{10} \quad (17)$$

$$k\nu = c_2(r_{20} - r_{10}) + r_{10}(c_2 - c_1) \quad (18)$$

$$r_{10}r_1\rho = k(c_2 - c_1) - P_2[r_2(r_{20} - r_{10}) + r_{10}(r_2 - r_1)] \quad (19)$$